JAERI-Research
98-010

FINITE BETA AND COMPRESSIBILITY EFFECTS ON STABILITY OF RESISTIVE MODES IN TOROIDAL GEOMETRY

March 1998

Jean-Noel G. LEBOEUF* and Gen-ichi KURITA

日本原子力研究所
Japan Atomic Energy Research Institute

本レポートは，日本原子力研究所が不定期に公刊している研究報告書です。
入手の問合わせは，日本原子力研究所研究情報部研究情報課（〒319-1195　茨城県那珂郡東海村）あて，お申し越しください。なお，このほかに財団法人原子力弘済会資料センター〒319-1195　茨城県那珂郡東海村日本原子力研究所内）で複写による実費領布をおこなっております。

This report is issued irregularly.
Inquiries about availability of the reports should be addressed to Research Information Division, Department of Intellectual Resources, Japan Atomic Energy Research Institure, Tokai-mura, Naka-gun, Ibaraki-ken 319-1195, Japan.

© Japan Atomic Energy Research Institute, 1998

編集兼発行　日本原子力研究所
印　　刷　㈱原子力資料サービス

Finite Beta and Compressibility Effects on Stability of Resistive Modes in Toroidal Geometry

Jean-Noel G. LEBOEUF* and Gen-ichi KURITA

Department of Fusion Plasma Research
Naka Fusion Research Establishment
Japan Atomic Energy Research Institute
Naka-machi, Naka-gun, Ibaraki-ken

(Received January 30, 1998)

Linear resistive stability results obtained from the toroidal magnetohydrodynamic codes FAR developed at the Oak Ridge National Laboratory in United States of America and AEOLUS developed at the Japan Atomic Energy Research Institute are compared for carefully constructed benchmark profiles and parameters. These are unstable to a tearing mode with toroidal mode number n=1. The eigenvalues and eigenfunctions calculated with both codes are in close agreement and show that the effect of compressibility is weak for these modes. The effect of finite plasma beta is considered, and the eigenvalues calculated by the FAR and AEOLUS codes also show good agreement. It is shown that the finite beta has a stabilizing effect on the toroidal tearing mode, but that the compressibility also has little effect on finite beta tearing modes.

Keywords: Tokamak, Linear Stability, Finite Beta, Compressibility, Resistive Tearing Modes, FAR, AEOLUS, Benchmark

* Oak Ridge National Laboratory

トロイダル配位における抵抗性モードの安定性に対する有限ベータと圧縮性の効果

日本原子力研究所那珂研究所炉心プラズマ研究部
Jean-Noel G. LEBOEUF*・栗田　源一

（1998年1月30日受理）

米国オーク・リッジ国立研究所で開発されたトロイダルMHDコードFARと日本原子力研究所で開発されたAEOLUSコードを使って注意深く作られたベンチマーク用の分布とパラメータに対して計算された線形の抵抗性MHD安定性の結果を比較した。これらの分布は、トロイダル・モード数n=1のテアリング・モードに対して不安定な分布である。双方のコードによって計算された、固有値と固有関数は非常に良く一致し、これらのモードに対して圧縮性の効果は弱いことが示された。FARコードとAEOLUSコードで計算された有限のプラズマ圧力の場合のテアリング・モードの成長率も良い一致を示した。有限ベータはトロイダル・テアリング・モードに対して安定化の効果を持つこと、また圧縮性の効果は有限ベータのテアリング・モードに対しても弱いことが示された。

那珂研究所：〒311-0193　茨城県那珂郡那珂町向山801-1
* オーク・リッジ国立研究所

Contents

目　　次

This is a blank page.

1. Introduction

The effect of compressibility on the stability of tokamak plasmas to magnetohydrodynamic (MHD) modes has generally been studied more in the context of ideal perturbations than of resistive ones. This is in part due to the small number of available tools to study such problems but more so engendered by the inherent difficulty in solving the full set of MHD equations in full toroidal geometry which includes the full effects of compressibility, both analytically and numerically [1-5].

Here, we investigate the inclusion of compressibility in the full set of MHD equations in the FAR and AEOLUS codes developed respectively at Oak Ridge National Laboratory. This study serves the purpose of providing an independent external benchmark for both models and their respective numerical implementations. It also serves the additional purpose of providing a study of the effect of compressibility on resistive tearing modes for a carefully controlled set of profiles and parameters. While the results reported here are limited to the effect of compressibility on the linear stability properties, these comparisons are clearly intended to include nonlinear stability as well.

The remainder of this report is organized as follows. The FAR and AEOLUS models are described in Sec. 2. The equilibria used for the comparisons are found in Sec. 3, while the results as to their stability to resistive MHD perturbations are described in Sec. 4. Finally, Sec. 5 serves as a summary and conclusion.

2. Models

The FAR code used in the present studies solves the full set of linear and nonlinear magnetohydrodynamic (MHD) equations, including parallel and perpendicular compressibility, in full toroidal geometry. Details on the formulation and numerics can be found in Refs. 1-2. FAR solves the full set of MHD equations in terms of potentials instead of primitive variables. The advantage of this formulation are the resulting second order derivatives which lead to more robust numerical properties than the first order derivatives present in a primitive variable formulation would. FAR calculates the linear and nonlinear stability of fixed boundary equilibria to ideal and resistive MHD modes. It does so in a straight field line coordinate system and uses finite differences in radius and sine/cosine Fourier mode expansions in poloidal and toroidal angles. In FAR, the linear

terms are treated implicitly in the time domain, which gives rise to the inversion of block tridiagonal matrices, while the nonlinear terms are treated explicitly in time and result in mode convolutions which are handled analytically instead of using fast Fourier transforms. Several limits have naturally been built into the FAR formulation. These range from incompressibility ($\nabla \cdot V=0$ and ratio of specific heats $\Gamma=\infty$) to finite compressibility or $\Gamma \neq 0$.

The AEOLUS codes used in the present studies include both a toroidally incompressible (or pressure convection version), named AEOLUS-IT, and a fully compressible one, named AEOLUS-FT. Details of the toroidally incompressible version can be found in Ref. 3. The representation is almost the same as in FAR. In fact, as stated in Ref. 1, the formulation adopted in FAR was based on the AEOLUS one. AEOLUS-IT uses potentials throughout while AEOLUS-FT uses potentials instead of magnetic fields but time evolution equations for the velocities in place of evolution equations for the poloidal θ and toroidal ϕ components of vorticity and $W = (\nabla \cdot V)$. In AEOLUS, as in FAR, the linear terms are treated implicitly, while the nonlinear terms are treated explicitly in the time domain. The convolutions arising from the nonlinear terms are also handled analytically.

3. Equilibria

The equilibria which are used as input to FAR are calculated by the two-dimensional, fixed boundary, and axisymmetric Grad-Shafranov solver RSTEQ which is described in Ref. 5. The equilibria which are used as input to AEOLUS have been either analytical or generated with the two-dimensional, free boundary, and axisymmetric MHD equilibrium code MEUDAS/SELENE which is described in Ref. 4.

The equilibrium considered for the comparisons of interest here is a circular one with inverse aspect ratio of 0.1 and with the following pressure P(r) and safety factor q(r) profiles:

$$P(r) = (1-(r/a)^2)^2,$$

$$q(r) = 1.38\ (1+(r/0.6)^8)^{1/4}.$$

This means that the q profile ranges from 1.38 at the plasma center to 3.85 at the plasma minor radius a. The value of poloidal beta is chosen to be $\beta_p=1$, unless otherwise noted. The equilibrium flux contours obtained with RSTEQ and MEUDAS/SELENE are plotted in Fig. 1. These plots confirm that the two calculated equilibria

are in very close agreement given that the Shafranov shifts and shapes are the same. The Shafranov shift dependence on poloidal beta values for equilibria used in FAR and AEOLUS codes are shown in Fig. 2. Although the shift for the FAR code is a little larger at high β_p than that of AEOLUS, they are in good agreement. In addition, Fig. 3 shows that the P and q profile obtained from RSTEQ are in excellent agreement with their analytical input. The agreement is also good between the RSTEQ profiles and the spline-interpolated P and q profiles used in FAR.

4. Linear Stability Results

The linear resistive stability calculations performed using FAR and AEOLUS-FT are carried out for toroidal mode number n=1 and 3 poloidal harmonics, namely m=1, m=2 ,and m=3. Up to 5 equilibrium n=0 modes have been included with m ranging from 0 to 4.

A uniform mesh covering the plasma minor radius is used with 400 grid points for FAR, while AEOLUS-FT uses a nonuniform mesh with a large number of grid points in the radial region ranging from around q=2 to around q=3 to insure greater accuracy and better convergence. The value of constant resistivity chosen for these comparisons corresponds to a Lundquist number S defined as $S=\tau_R/\tau_{pA}$ of 10^5, where the poloidal Alfvén time $\tau_{pA} = a/v_{pA}$, with v_{pA} the poloidal Alfvén velocity defined with the edge poloidal magnetic field $B_\theta(a)$.

The dynamical n=1 modes are perturbed ab initio and are converged in time to their linear toroidal eigenvalue for the growth rate (this mode is purely growing) and respective eigenfunctions. The eigenfunctions obtained with the fully compressible FAR for $\Gamma=5/3$ are shown in Fig. 4 for the perturbed poloidal stream function ϕ, the poloidal velocity, the poloidal flux ψ, the poloidal magnetic field, the electrostatic potential α, and the pressure P, for the poloidal mode numbers m=1, 2, and 3. These same eigenfunctions are shown in Fig. 5 but for AEOLUS-FT and again for $\Gamma=5/3$. Agreement between AEOLUS and FAR with full compressibility is quite remarkable as far as details of the eigenfunctions are concerned. The difference between profiles of the electrostatic potential α in Figs.4 and 5, is attributed to the definition of α; in Fig. 4, it is redefined, while in Fig. 5, the definition is a original one. The corresponding eigenfunctions obtained with FAR but with incompressibility imposed (see Refs. 1 and 2 for further details) and with AEOLUS-FT are shown in Figs. 6 and 7, respectively. Comparison of these three figures indicates that the effect of

compressibility for these resistive tearing modes (at the values of aspect ratio and β_p considered) is rather weak and in fact only noticeable in the details.

A comparison of the growth rates, normalized to τ_{pA}, is presented in Fig. 8 for FAR and AEOLUS-FT with varying values of the compressibility parameter (ratio of specific heats) Γ. The number of grid points used in AEOLUS-FT was 500, packed around the q=2 and q=3 rational surfaces. The growth rates obtained with AEOLUS-FT, which are well converged in terms of the number of grid points used, are slightly higher than those obtained in FAR (which are also well converged in the number of grid points used, namely 400 uniformly distributed radial grid points). In addition, the growth rate obtained with FAR exhibits less of a variation with Γ than the growth rate obtained with AEOLUS-FT which tends to decrease slightly with Γ. These minor differences, however, are almost negligible.

In the following, we investigate the finite beta effect on resistive MHD mode, and also make comparisons between the results obtained with both the FAR and AEOLUS-FT codes. The growth rate dependence on β_p values is shown in Fig.9, for two values of specific heat ratio, Γ= 5/3 and 1000. The growth rates in the figure are calculated with the FAR code, and shows a clear stabilizing effect of the finite plasma beta on toroidal resistive modes. There appears to be two kinds of stabilizing effects, one is around β_p=0 and the other is mainly in the high β_p region. The reduction of the growth rate is very steep near β_p=0, especially in the Γ=1000 case, while in the high β_p region, it appears gradually. The reduction around β_p=0 comes from the compressional wave damping, and it is absent in the case of β_p=0 or in the calculation using the toroidal incompressible resistive MHD equations[3] or the reduced set of resistive MHD equations using the assumption of tokamak ordering, $a/R_0 \ll 1$[6]. The ratio of the growth rate of compressible case at β_p=0 to incompressible case near β_p=0 in Fig.9 is about 1.6, which is just consistent with analytical calculation in the case of large aspect ratio [7-9].

The comparison of the dependence of the growth rate on β_p for two values of Γ is shown in Fig.10, for Γ=5/3 in Fig.10.a and $\Gamma=10^3$ in Fig.10.b. To show the coincidence more clearly around β_p = 0, we use a logarithmic scale for the β_p values in the figure. Excellent agreement can be seen for both cases. A little disagreement in the high β_p region must come mainly from the difference of equilibria. As mentioned before, the equilibria are obtained numerically in FAR code, while they are obtained analytically in the AEOLUS code using an expansion in inverse aspect ratio.

5. Summary

The linear studies presented in this report show that the fully compressible versions of the MHD stability codes FAR and AEOLUS give results that are in close agreement in the case on n=1 resistive tearing modes. This agreement is particularly remarkable in the eigenfunctions. Both FAR and AEOLUS show that the effect of compressibility is rather weak for these resistive tearing modes. The effect of finite plasma beta has also been considered, and the eigenvalues calculated with the FAR and AEOLUS codes also show good agreement. It is shown that finite beta has stabilizing effect on the toroidal tearing mode, but that compressibility also has little effect on finite beta tearing modes.

Nonlinear comparisons do however remain to be made between FAR and AEOLUS, if only to assess the consequences of compressibility on the nonlinear evolution of such resistive modes.

Acknowledgments

The authors would like to acknowledge Drs. T. Tuda, M. Azumi and T. Hirayama for useful discussions and continuing encouragement. Jean-Noel Leboeuf would like to acknowledge the JAERI Foreign Researcher Inviting Program for making this visit possible. He would also like to thank all of the members of the Plasma Theory Laboratory, Department of Fusion Plasma Research, Naka Fusion Research Establishment for their generous help and hospitality during his visit at Naka.

References

1. L. A. Charlton, J. A. Holmes, H. R. Hicks, V. E. Lynch, and B. A. Carreras, "Numerical calculations using the full MHD equations in toroidal geometry", Journal of Computational Physics **63**, 107-139 (1986).

2. L. A. Charlton, J. A. Holmes, V. E. Lynch, B. A. Carreras, and T. C. Hender, "Compressible linear and nonlinear resistive MHD calculations in toroidal geometry", Journal of Computational Physics **86**, 270-293 (1990).

3. G. Kurita, M. Azumi, and T. Takeda, " 'AEOLUS-IT' MHD simulation code based on a toroidally incompressible plasma model", Report No. JAERI-M 93-004, Japan Atomic Energy Research Institute (JAERI), February 1993.

4. M. Azumi, G. Kurita, T. Matsuura, T. Takeda, Y. Tanaka, and T. Tsunematsu, "A fluid model numerical code system for tokamak fusion research", Proceedings, Fourth Symposium on the Computing Methods in Applied Sciences and Engineering, Paris, 1979, Computing Methods in Applied Sciences and Engineering, R. Glowinski, J. L. Lyons (editors), North Holland Publishing Company, 1980, pp. 335-356.

5. V. E. Lynch, B. A. Carreras, H. R. Hicks, J. A. Holmes, and L. Garcia, "Resistive MHD studies of High β tokamak plasmas", Computer Physics Communications **24**, 465-476 (1981).

6. G. Kurita, M. Azumi, T. Tsunematsu and T. Takeda, "Numerical Studies of Toroidal Coupling on Low-m Resistive Modes", Plasma Physics **25**, 1097-1112 (1983).

7. H.P. Furth, P.H. Rutherford and H. Selberg, "Tearing Mode in the Cylindrical Tokamak", Physics of Fluids **16**, 1054-1063 (1973).

8. A.H. Glasser, J.M. Greene and J.L. Johnson, "Resistive Instabilities in General Toroidal Plasma Configurations", Physics of Fluids **18**, 875-888 (1975).

9. T.C. Hender, R.J. Hastie and D.C. Robinson, "Finite Beta Effects on Tearing Modes in the Tokamak", Nuclear Fusion **27**, 1389-1400 (1987).

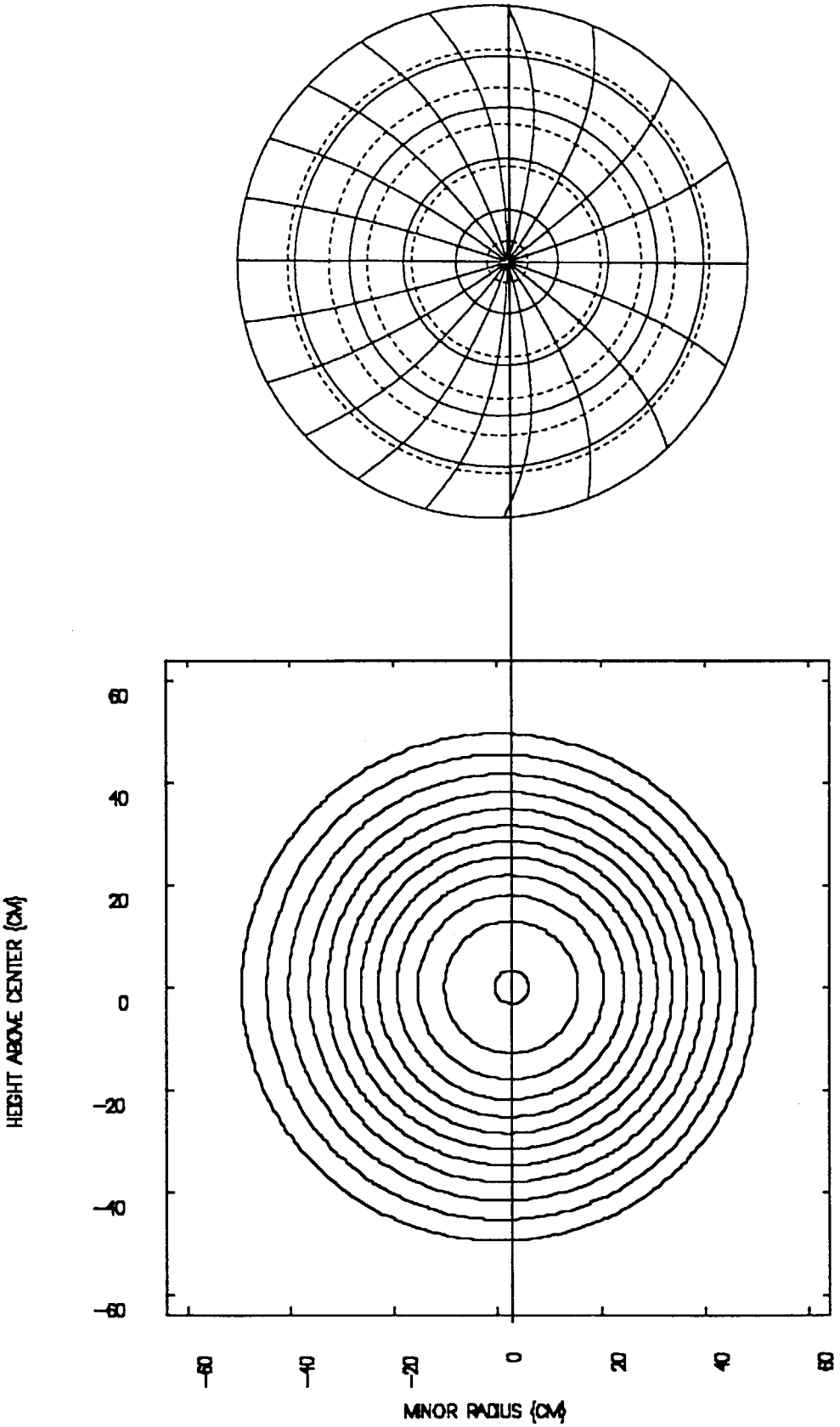

Fig. 1. Equilibrium flux surfaces for β_p=1 calculated with MEUDAS (top) and RSTEQ (bottom). Note the good agreement in the shape and the shift.

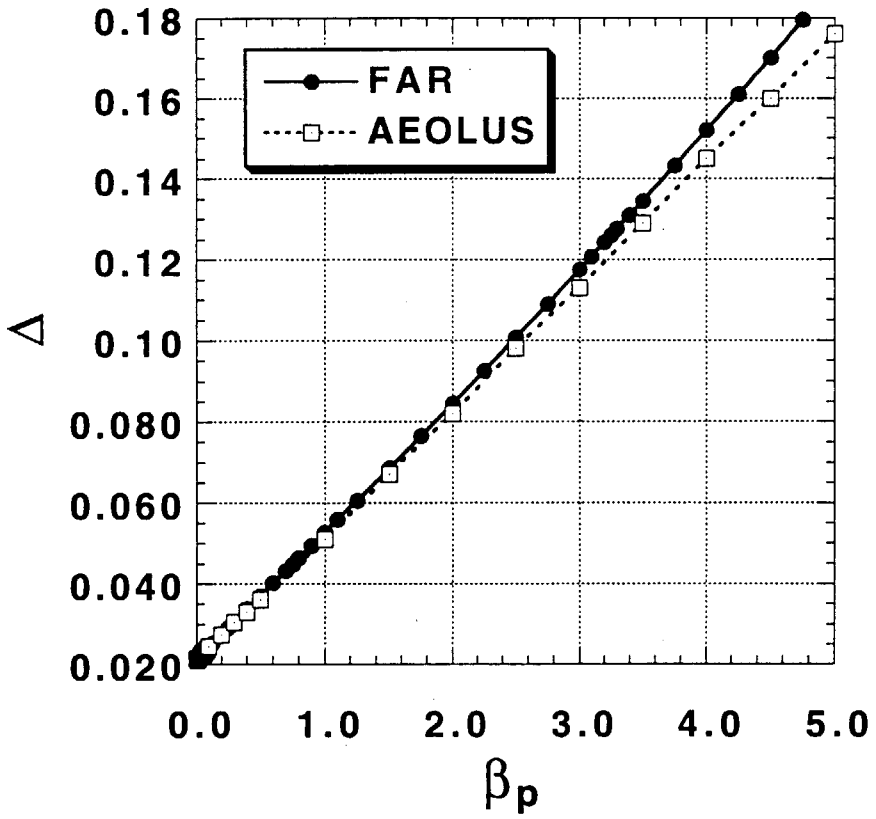

Fig. 2. Shafranov shift dependence on poloidal beta value of equilibria obtained by RSTEQ for FAR and MEUDAS for AEOLUS.

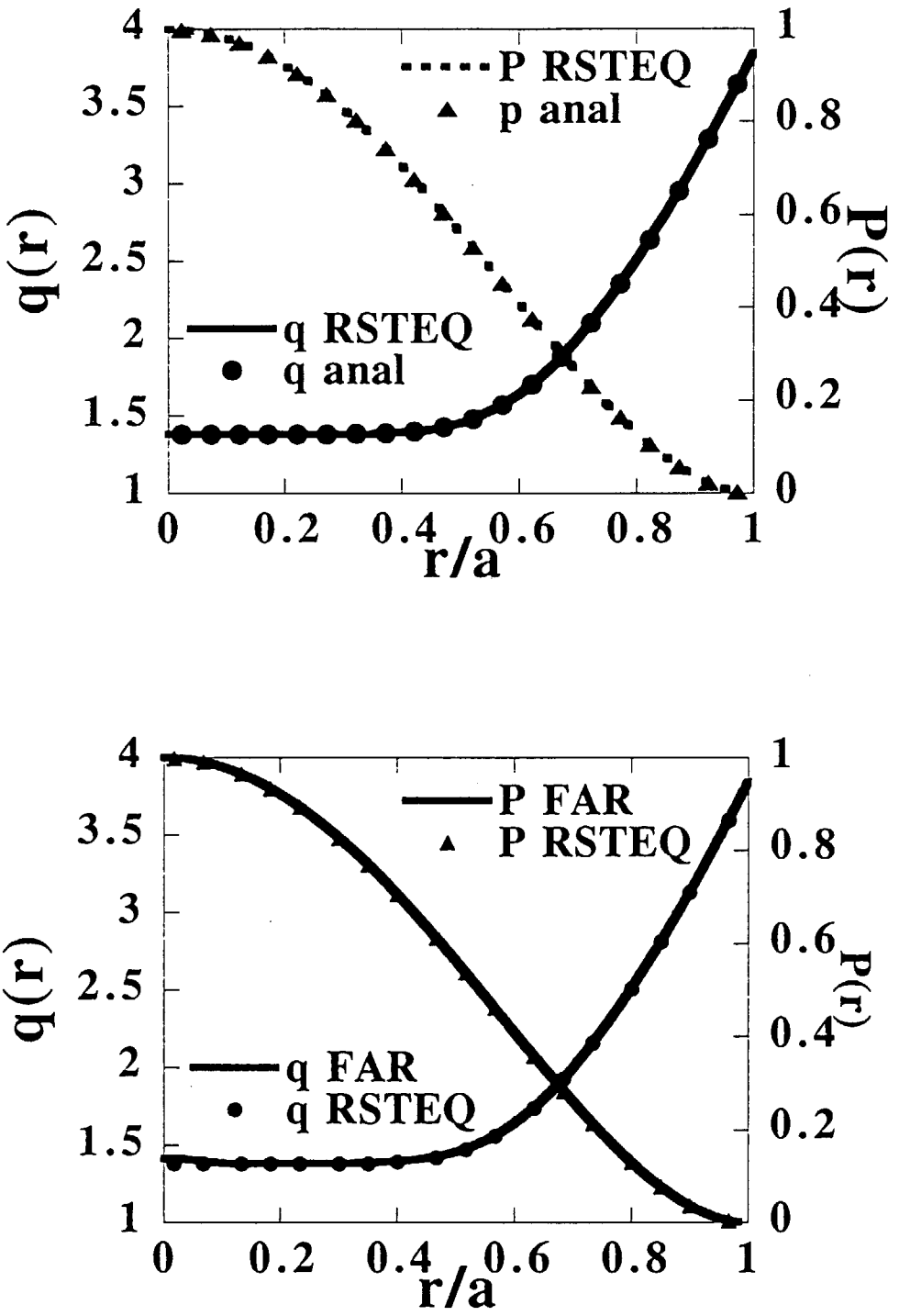

Fig. 3. a) Comparison of analytic pressure P and safety factor q profiles with profiles calculated with the 2D Grad-Shafranov solver RSTEQ. b) Comparison of equilibrium P and q profiles from RSTEQ and as reconstructed in FAR.

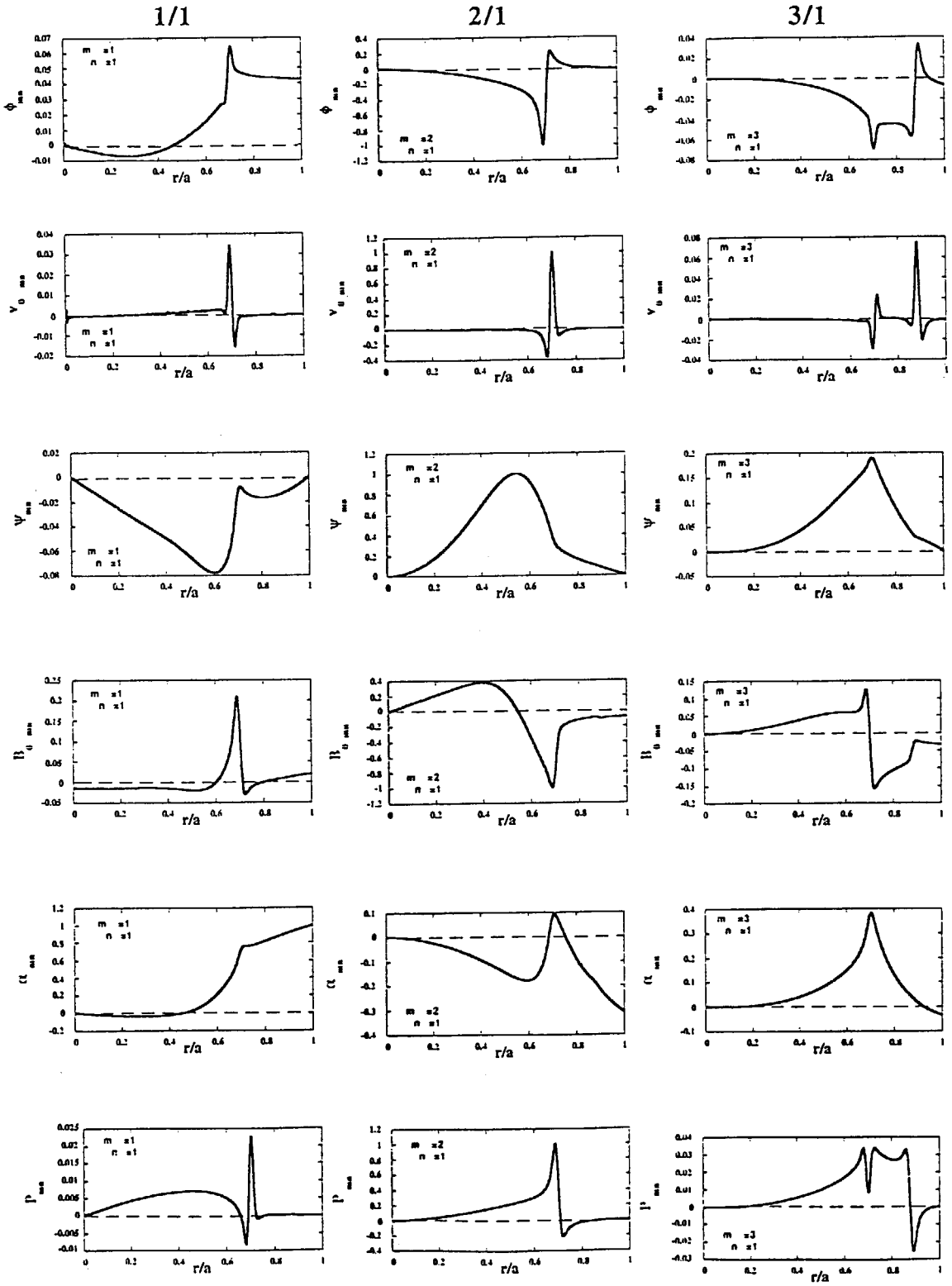

Fig. 4. Radial profiles of the m=1, 2, and 3 poloidal components of the toroidal mode number n=1 toroidal eigenmode for electrostatic potential f, θ component of the velocity, poloidal flux ψ, θ component of the magnetic field, α, and pressure P, obtained with the full MHD code FAR with Γ=5/3.

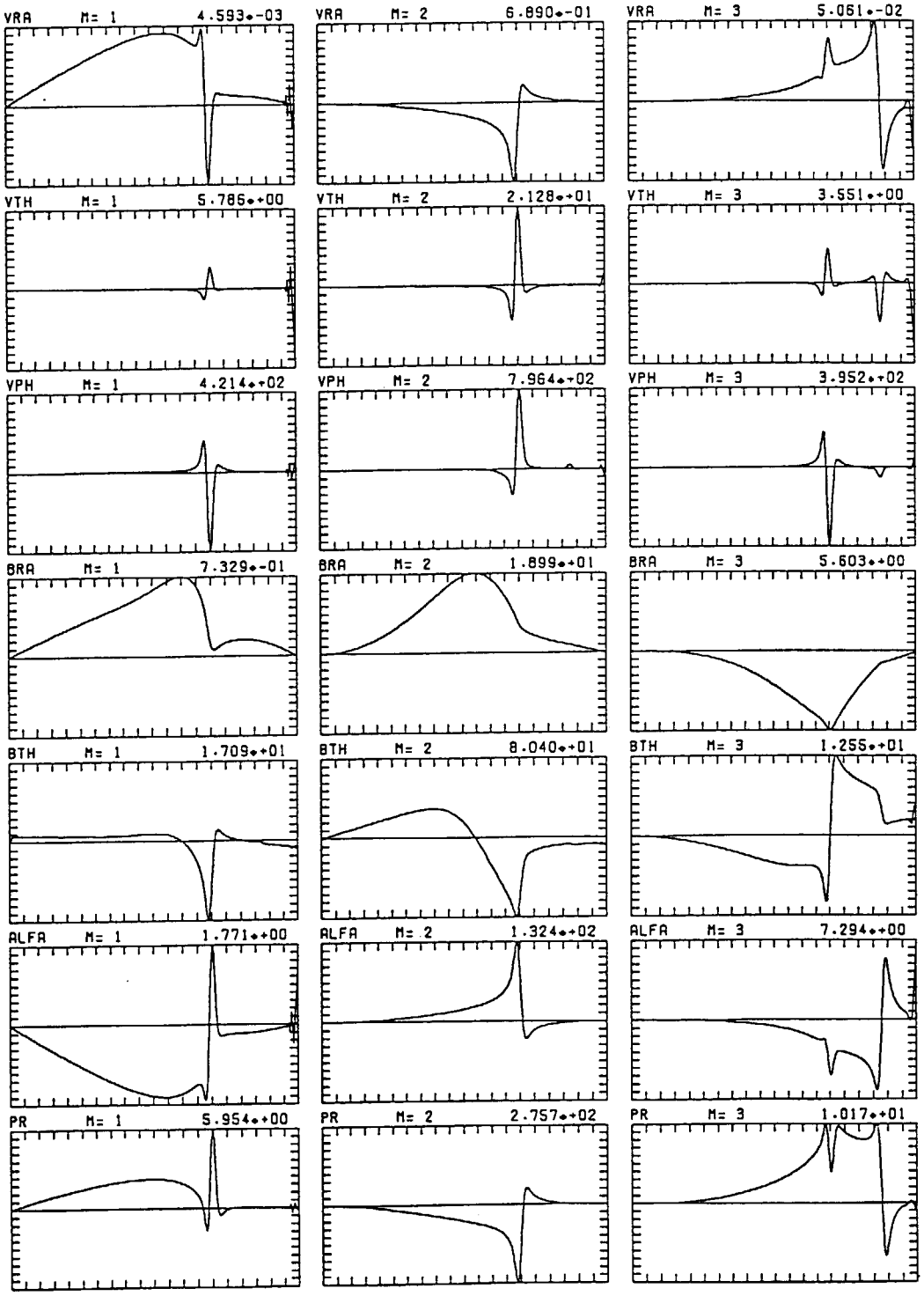

Fig. 5. Radial profiles of the m=1, 2, and 3 poloidal components of the n=1 toroidal eigenmode for minor radial, poloidal and toroidal components of the velocity, poloidal flux ψ, θ component of the magnetic field, α, and pressure P, obtained with the compressible MHD code AEOLUS-FT with $\Gamma = 5/3$.

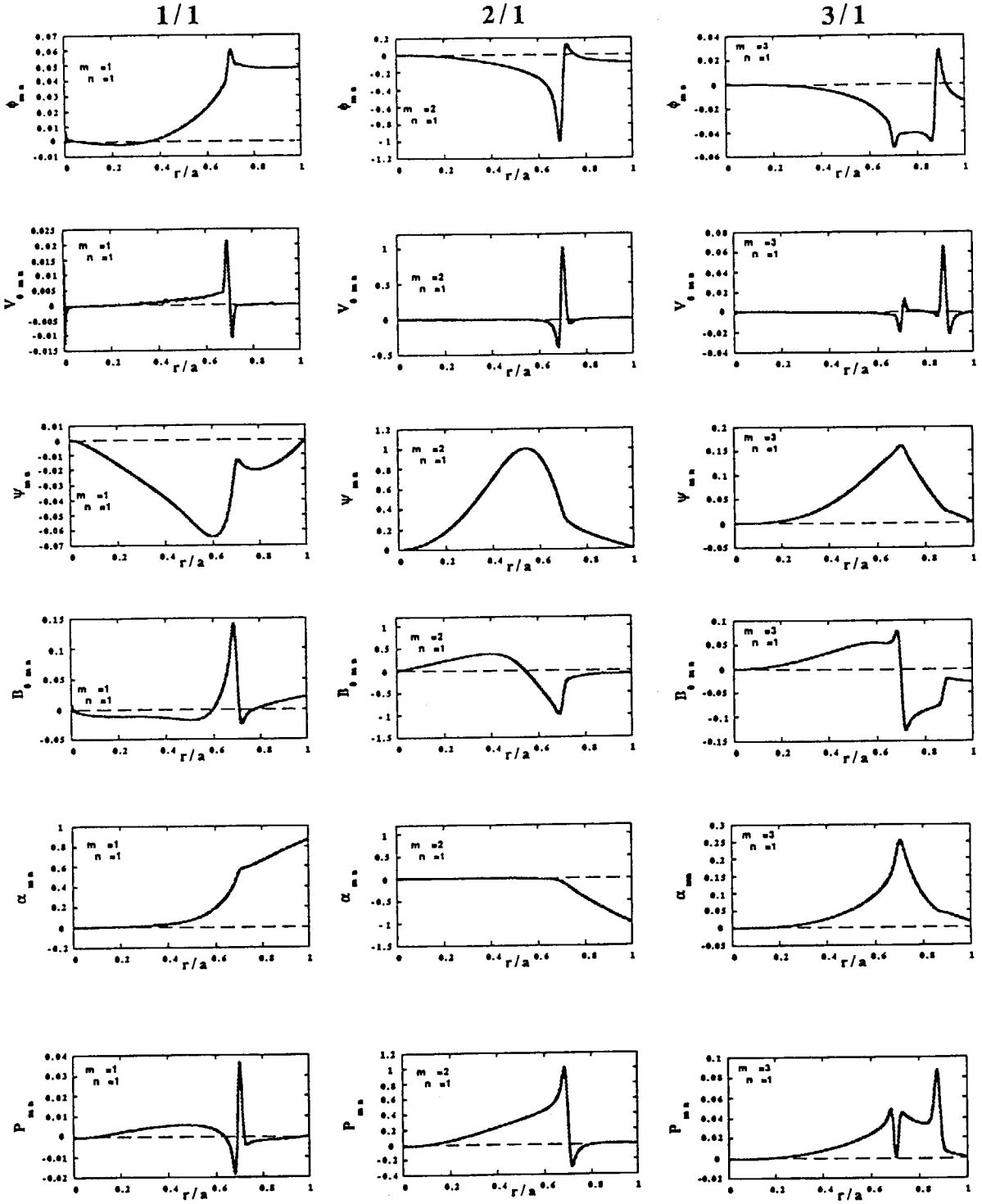

Fig. 6. Radial profiles of the m=1, 2, and 3 poloidal components of n=1 toroidal eigenmode for electrostatic potential ϕ, θ component of the velocity, poloidal flux ψ, θ component of the magnetic field, α, and pressure P, obtained with the MHD code FAR in the incompressible limit ($\Gamma = 10^3$).

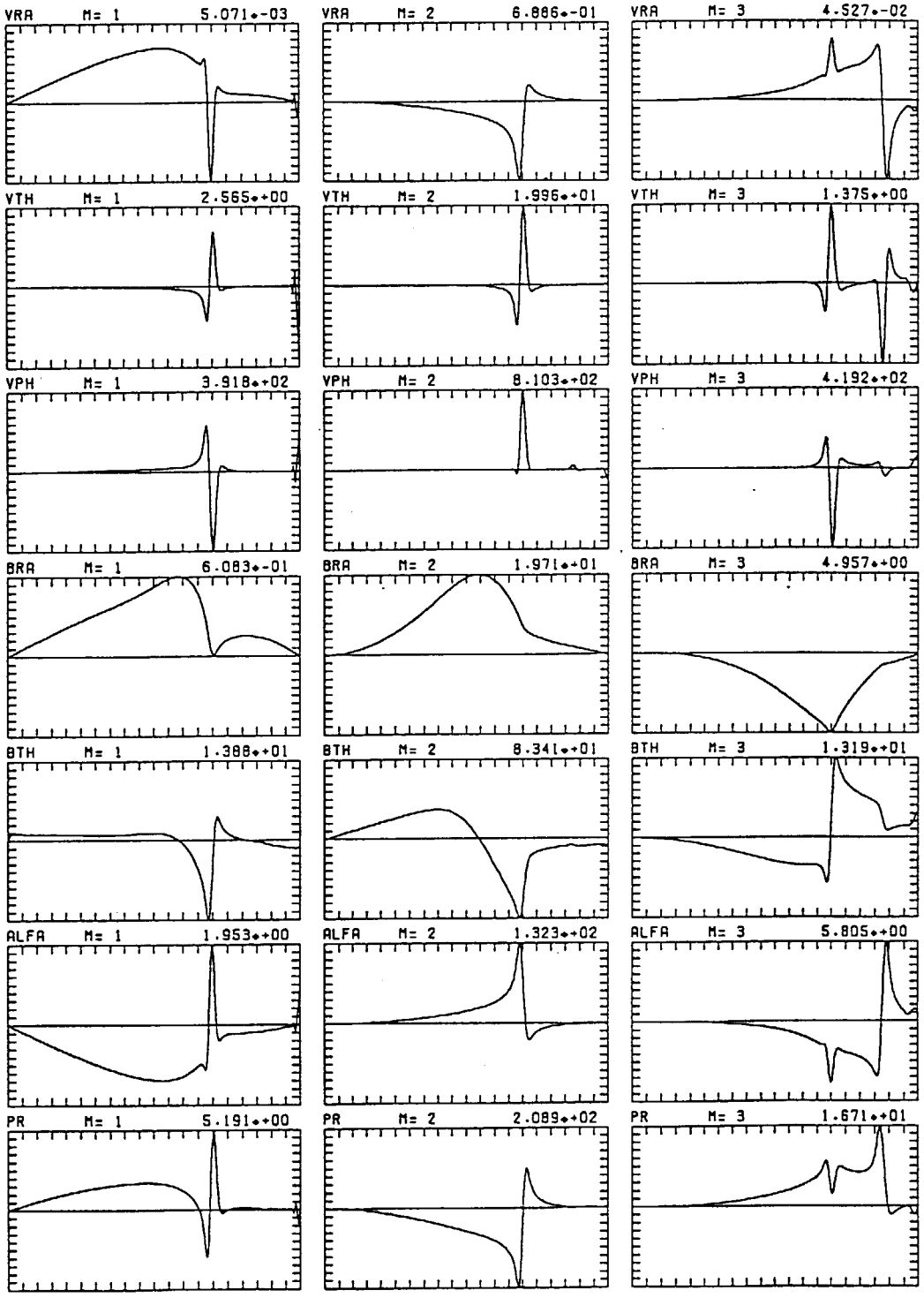

Fig. 7. Radial profiles of the m=1, 2, and 3 poloidal components of the n=1 toroidal eigenmode for minor radial, poloidal and toroidal components of the velocity, poloidal flux ψ, θ component of the magnetic field, α, and pressure P, obtained with the compressible MHD code AEOLUS-FT in the incompressible limit ($\Gamma = 10^3$).

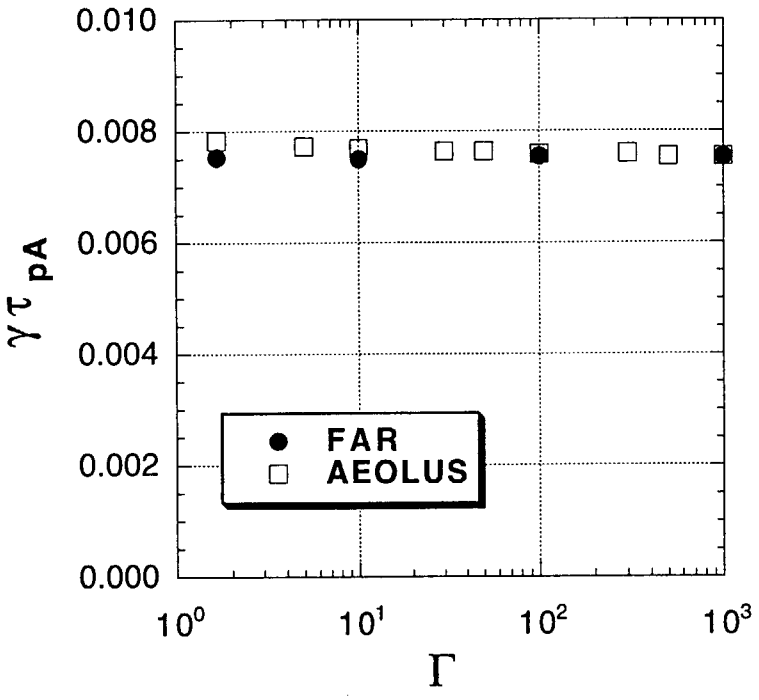

Fig. 8. Growth rates normalized to the poloidal Alfvén time $\tau_{pA}=a/V_\theta(a)$ for the n=1 resistive mode with $S=\tau_R/\tau_{pA}=10^5$ at the q=2 rational surface ($r_s/a=0.7$) obtained with the full MHD FAR and AEOLUS-FT codes and various values of Γ.

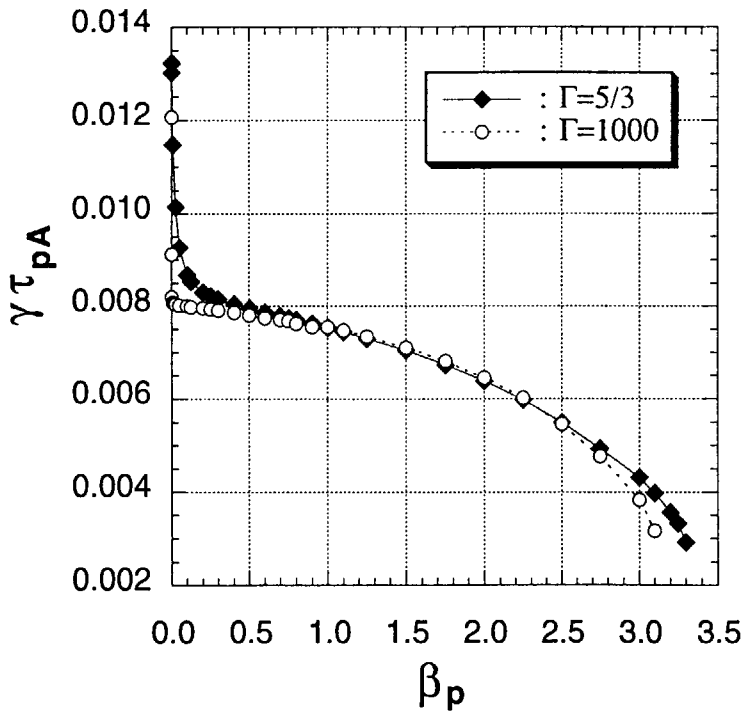

Fig. 9. Growth rates dependence on β_p normalized to the poloidal Alfvén time $\tau_{pA}=a/V_\theta(a)$ for the n=1 resistive mode obtained with the full MHD FAR code for two values of Γ.

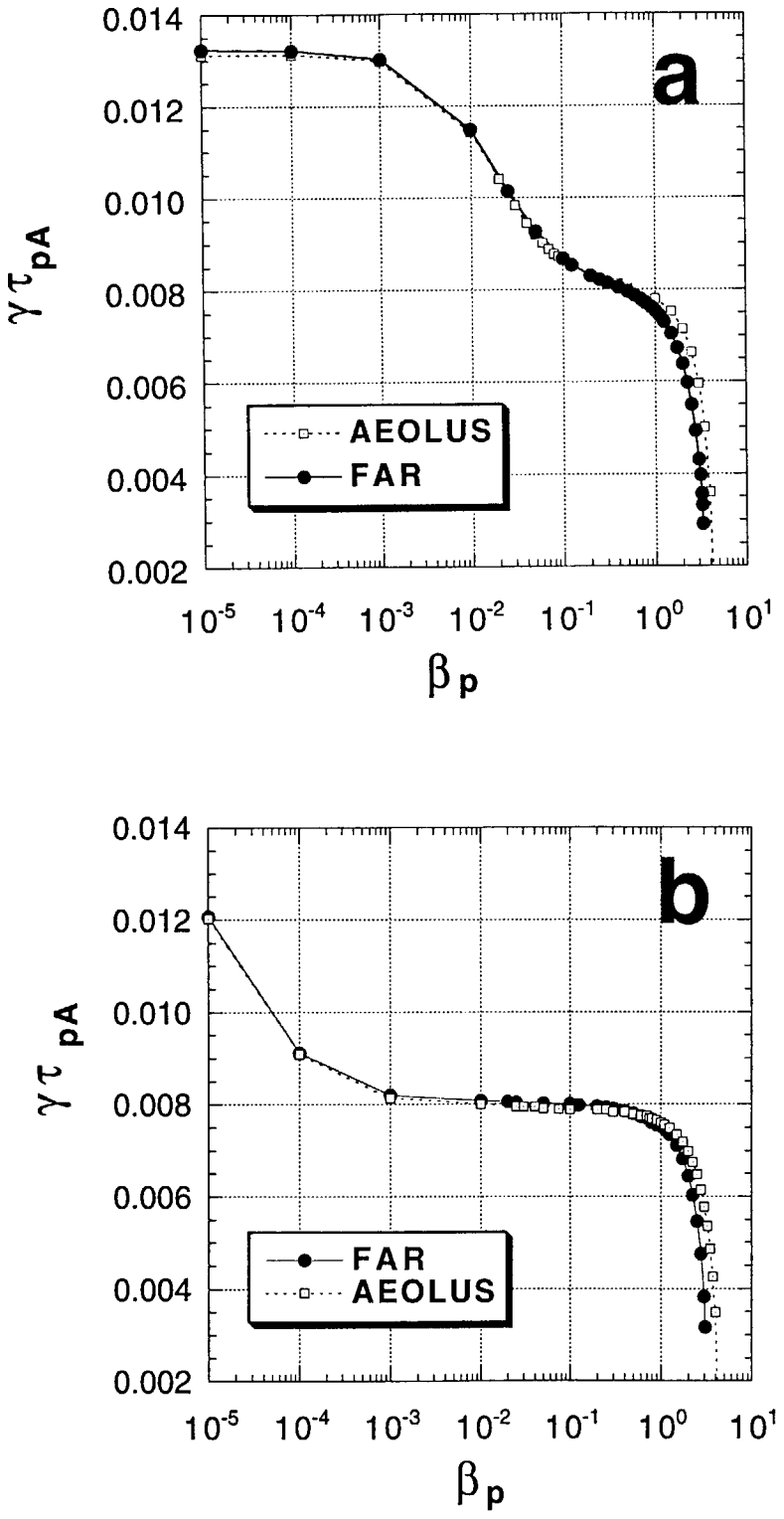

Fig. 10. Comparisons of growth rates dependence on β_p for the n=1 resistive tearing mode obtained with the full MHD FAR and AEOLUS codes for a) Γ =5/3 and b) Γ =10^3.

This is a blank page.

国際単位系 (SI) と換算表

表 1　SI基本単位および補助単位

量	名称	記号
長さ	メートル	m
質量	キログラム	kg
時間	秒	s
電流	アンペア	A
熱力学温度	ケルビン	K
物質量	モル	mol
光度	カンデラ	cd
平面角	ラジアン	rad
立体角	ステラジアン	sr

表 2　SIと併用される単位

名称	記号
分，時，日	min, h, d
度，分，秒	°, ′, ″
リットル	l, L
トン	t
電子ボルト	eV
原子質量単位	u

1 eV = 1.60218 × 10^{-19} J

1 u = 1.66054 × 10^{-27} kg

表 5　SI接頭語

倍数	接頭語	記号
10^{18}	エクサ	E
10^{15}	ペタ	P
10^{12}	テラ	T
10^{9}	ギガ	G
10^{6}	メガ	M
10^{3}	キロ	k
10^{2}	ヘクト	h
10^{1}	デカ	da
10^{-1}	デシ	d
10^{-2}	センチ	c
10^{-3}	ミリ	m
10^{-6}	マイクロ	μ
10^{-9}	ナノ	n
10^{-12}	ピコ	p
10^{-15}	フェムト	f
10^{-18}	アト	a

表 3　固有の名称をもつSI組立単位

量	名称	記号	他のSI単位による表現
周波数	ヘルツ	Hz	s^{-1}
力	ニュートン	N	$m \cdot kg/s^2$
圧力，応力	パスカル	Pa	N/m^2
エネルギー，仕事，熱量	ジュール	J	N·m
工率，放射束	ワット	W	J/s
電気量，電荷	クーロン	C	A·s
電位，電圧，起電力	ボルト	V	W/A
静電容量	ファラド	F	C/V
電気抵抗	オーム	Ω	V/A
コンダクタンス	ジーメンス	S	A/V
磁束	ウェーバ	Wb	V·s
磁束密度	テスラ	T	Wb/m^2
インダクタンス	ヘンリー	H	Wb/A
セルシウス温度	セルシウス度	℃	
光束	ルーメン	lm	cd·sr
照度	ルクス	lx	lm/m^2
放射能	ベクレル	Bq	s^{-1}
吸収線量	グレイ	Gy	J/kg
線量当量	シーベルト	Sv	J/kg

表 4　SIと共に暫定的に維持される単位

名称	記号
オングストローム	Å
バーン	b
バール	bar
ガル	Gal
キュリー	Ci
レントゲン	R
ラド	rad
レム	rem

1 Å = 0.1 nm = 10^{-10} m

1 b = 100 fm^2 = 10^{-28} m^2

1 bar = 0.1 MPa = 10^5 Pa

1 Gal = 1 cm/s^2 = 10^{-2} m/s^2

1 Ci = 3.7 × 10^{10} Bq

1 R = 2.58 × 10^{-4} C/kg

1 rad = 1 cGy = 10^{-2} Gy

1 rem = 1 cSv = 10^{-2} Sv

（注）

1. 表1～5は「国際単位系」第5版，国際度量衡局 1985年刊行による。ただし，1 eVおよび1 uの値はCODATAの1986年推奨値によった。
2. 表4には海里，ノット，アール，ヘクタールも含まれているが日常の単位なのでここでは省略した。
3. barは，JISでは流体の圧力を表わす場合に限り表2のカテゴリーに分類されている。
4. EC閣僚理事会指令ではbar，barnおよび「血圧の単位」mmHgを表2のカテゴリーに入れている。

換　算　表

力	N(=10^5 dyn)	kgf	lbf
	1	0.101972	0.224809
	9.80665	1	2.20462
	4.44822	0.453592	1

粘度　1 Pa·s(N·s/m^2) = 10 P(ポアズ)(g/(cm·s))

動粘度　1 m^2/s = 10^4 St(ストークス)(cm^2/s)

圧力	MPa(=10 bar)	kgf/cm^2	atm	mmHg(Torr)	lbf/in^2(psi)
	1	10.1972	9.86923	7.50062 × 10^3	145.038
	0.0980665	1	0.967841	735.559	14.2233
	0.101325	1.03323	1	760	14.6959
	1.33322 × 10^{-4}	1.35951 × 10^{-3}	1.31579 × 10^{-3}	1	1.93368 × 10^{-2}
	6.89476 × 10^{-3}	7.03070 × 10^{-2}	6.80460 × 10^{-2}	51.7149	1

エネルギー・仕事・熱量	J(=10^7 erg)	kgf·m	kW·h	cal(計量法)	Btu	ft·lbf	eV
	1	0.101972	2.77778 × 10^{-7}	0.238889	9.47813 × 10^{-4}	0.737562	6.24150 × 10^{18}
	9.80665	1	2.72407 × 10^{-6}	2.34270	9.29487 × 10^{-3}	7.23301	6.12082 × 10^{19}
	3.6 × 10^6	3.67098 × 10^5	1	8.59999 × 10^5	3412.13	2.65522 × 10^6	2.24694 × 10^{25}
	4.18605	0.426858	1.16279 × 10^{-6}	1	3.96759 × 10^{-3}	3.08747	2.61272 × 10^{19}
	1055.06	107.586	2.93072 × 10^{-4}	252.042	1	778.172	6.58515 × 10^{21}
	1.35582	0.138255	3.76616 × 10^{-7}	0.323890	1.28506 × 10^{-3}	1	8.46233 × 10^{18}
	1.60218 × 10^{-19}	1.63377 × 10^{-20}	4.45050 × 10^{-26}	3.82743 × 10^{-20}	1.51857 × 10^{-22}	1.18171 × 10^{-19}	1

1 cal = 4.18605 J(計量法)

= 4.184 J　(熱化学)

= 4.1855 J　(15 °C)

= 4.1868 J(国際蒸気表)

仕事率　1 PS(仏馬力)

= 75 kgf·m/s

= 735.499 W

放射能	Bq	Ci
	1	2.70270 × 10^{-11}
	3.7 × 10^{10}	1

吸収線量	Gy	rad
	1	100
	0.01	1

照射線量	C/kg	R
	1	3876
	2.58 × 10^{-4}	1

線量当量	Sv	rem
	1	100
	0.01	1

(86年12月26日現在)

FINITE BETA AND COMPRESSIBILITY EFFECTS ON STABILITY OF RESISTIVE MODES IN TOROIDAL GEOMETRY